6. Stewart J. J. P. Optimization of parameters for semiempirical methods II // J. Comp. Chem. 1991. Vol. 10. № 2. P. 221–264.

7. Stewart J. J. P. Comparison of the accuracy of semiempirical and some DFT methods for predicting heats of formation // J. Comp. Chem. 2004. Vol. 10. P. 6–12.

8. Stuart J. J. P. Optimization of parameters for semiempirical methods V: Modification of NDDO approximations and application to 70 elements // J. Mol. Model. 2007. Vol. 13. P. 1172–1213.

9. Shimomura O. Bioluminescence. Chemical Principles and Methods. World Scientific Publishing Co. Pte. Ltd., 2006.

10. Shimomura O. The discovery of aequorin and green fluorescent protein // J. of Microscopy. 2005. Vol. 217. P. 3–15.

11. Renilla luciferin as the substrate for calcium induced photoprotein bioluminescence. Assignment of luciferin tautomers in aequorin and mnemiopsin / K. Hori, J. M. Anderson, W. W. Ward, M. J. Cormier // Biochemistry. 1975. Vol. 14. № 11. P. 2371–2376.

L. Yu. Antipina, S. G. Ovchinnikov

QUANTUM-CHEMICAL STUDY OF COELENTERAZINE WITH THE ACCOUNT OF ENVIRONMENT AND ELECTRONIC CORRELATIONS

Electronic structure and total energy of various isomeric forms of coelenterazine has been calculated by methods of quantum chemistry both in one-electronic approach, and with correlation effects. It is shown that the account of electronic correlations allows choosing structure of coelenterazine CLZ (1H) as most probable of possible isomeric forms.

Keywords: obelin, quantum-chemical calculations, coelenterazine, bioluminescence, electronic correlation.

© Антипина Л. Ю., Овчинников С. Г., 2011

УДК 539.21:537.86

S. S. Aplesnin, O. B. Romanova, A. S. Krylov, Hsiang-Lin Liu, I. V. Aldashev

RESEARCH OF RAMAN SPECTRA IN Co$_x$Mn$_{1-x}$S SOLID SOLUTIONS*

Temperature dependence of Raman spectra in the frequency interval 100...1 200 cm^{-1} in the 100...300 K range temperature has been investigated in the substance of Co$_x$Mn$_{1-x}$S solid solutions. A Raman spectra study has uncovered evidence of strong orbital fluctuations that manifest itself in kind of composite line shape at ω_2 = 273...298 cm^{-1}, arisen from splitting of phonon modes with different temperature dependences of the intensity below the orbital ordering transition.

Keywords: magnetically ordered materials, Raman spectra, spin-orbit effects, orbital fluctuations, sulfides.

An active role of orbital degree of freedom in the lattice [1] and the electronic response can be most typically seen in manganese oxide compounds with perovskite structure [2–4]. A more transparent example is the case of RTiO$_3$ [5] and RVO$_3$ [6; 7] with 3d_1 and 3d_2 electron configuration, respectively, both retaining the orbital degree of freedom in the t$_{2g}$ state. The actual orbital order pattern in these t$_{2g}$ electron systems is not straightforwardly visible from the crystal structure alone because of the relatively weak Jahn–Teller (JT) distortion of the t$_{2g}$ electron. An example of dynamical orbital correlation is seen in the spin-state transition in LaCoO$_3$ with 3d_6 configuration of Co [8]. In fact, the correlated local lattice distortion clearly shows up in the infrared phonon spectra in accord with the spin-state crossover [9], although the average lattice structure appears to be undistorted from that of the ground state. However, LaCoO$_3$ undergoes the insulator-to-metal transition by warming above 500 K. As predicted by the LDA calculation [8], this phenomenon may be interpreted as the loss of the orbital (short-range) order.

Charge-orbital order can arise from to redistribution of electron density between orbitales and as a results of electron-lattice interaction induces an anomalous change in the phonons frequency and the linewidth. The Raman background can give information of the electronic excitations. The change of the diffusive Raman scattering in the paramagnetic phase has been attributed to the change of the lattice vibrations and their correlation to the electron structure. A detailed investigation of the electronic and lattice excitations is therefore crucial for the understanding of origin of strong coupling between charge, lattice and spin degrees of freedom of the Co$_x$Mn$_{1-x}$S solid solutions.

---

*This study was supported by the Russian Foundation for Basic Research project № 09-02-00554_a; № 09-02-92001-NNS_a; ADTP “Development of scientific potential of the higher school” № 2.1.1/401.

The occupancy of the orbitals and the orbital order can cause to change in the static and dynamic properties of structure. Raman spectroscopy proved to be a useful tool for the study of structural phase transitions. Materials presenting perovskite crystal structure, with a large number of structural changes, have been extensively studied by this technique [10]. A broadening of the phonon peaks, associated to the lattice disorder and the presence of a central mode near and above the transition temperature is observed at the order-disorder transitions. Raman-scattering studies are used for study of the JT transition in $LaMnO_3$ [11] and for polycrystalline α-MnSe samples [12]. α-MnSe has a NaCl-type structure with O_h symmetry and only one infrared (IR) active mode of F_{1u} symmetry. The rock salt structure has no Raman active modes, but there are three irreducible components A_{1g}, T_{2g} and E_g of a second-rank tensor. All combinations of modes can be observed in unpolarized measurements on the polycrystalline samples, i. e., summation bands, difference bands (at low temperatures) and overtones [13]. Transition energy $^6A_1$–$^4T_2$ depends on spin and orbital ordering and on spin and phonon dynamics. The measurements were made with a Horiba Jobin Yvon T64000 Raman spectrometer. The Raman spectra taken in the temperature range 140…300 K at the frequencies 100…750 cm^{-1} are given in fig. 1. At room temperature, the spectra are obtained in the wider frequency band 100…1 200 cm^{-1}. At the frequencies ω_1 = 115 cm^{-1}, ω_2 = 273…298 cm^{-1}, and ω_3 = 840 cm^{-1} the active Raman modes are observed. According to the literature data [12], positioning two peaks at the frequencies ω_1 = 115 cm^{-1} and ω_2 = 260 cm^{-1} for MnS is related to transverse optical mode TO(X) and the combination of optical and acoustic phonon modes TO + LA(X). The Debye temperature for MnS is T_D = 230 K and the corresponding frequency is ω_D = 165 cm^{-1}. In the MnS the third peak at the frequency ω_3 = 840 cm^{-1} is absent and this hump may be attributed to polaron, a collision-dominated response, or a plasmalike excitation. A similar broad peak around 1 200 cm^{-1} is observed in $La_{1-x}Sr_xMnO_3$ and was explained by a polaron excitation [14].

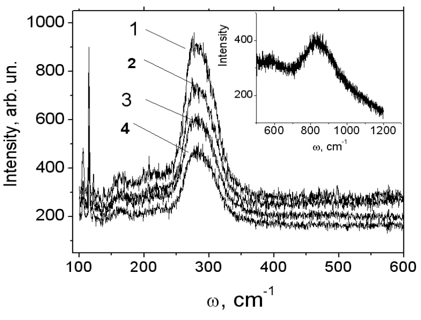

Fig. 1. Raman spectra versus frequency at temperatures of 160 K (1), 210 K (2), 230 K (3), and 250 K (4) for the $Co_{0.05}Mn_{0.95}S$ sample. The inset presents the Raman spectra taken at T = 300 K for the same sample

The weak feature in I (ω) is observed at frequency 163 cm^{-1} to be temperature dependent, but the quality of spectra did not allow a quantitative analysis. Because isomorphic crystals MnS have the values of exchange energies, dipolar anisotropy and acoustic magnon [15] in the same range as α-MnSe, the mode frequency 163 cm^{-1} could be a combination of TO mode and acoustic one-magnon as α-MnSe: $\omega_{LTO}(\Gamma) + \omega_{1Mac}$ = = 138 cm^{-1} + 18 cm^{-1} = 156 cm^{-1}.

With a decrease in temperature below T < 240 K, the peak at ω_2 becomes asymmetric and may be presented as a two peaks at the frequencies $\omega_{2,1} \approx$ 273 cm^{-1}, $\omega_{2,2} \approx$ 296 cm^{-1} that is illustrated in fig. 2. The temperature dependence of $Co_xMn_{1-x}S$ Raman spectra is similar to spectra observed in $CaMnO_3$ [16]. The linewidth for the 260 cm^{-1} modes in $CaMnO_3$ could not be measured above 520 K, due to the large overlapping of both peaks. This compound presents the orthorhombic P_{nma} perovskite crystal structure with Mn^{+4} ions and a Jahn–Teller distortion of oxygen octahedral is not observed.

The composite form of Raman spectra at ω_2 = 273…298 cm^{-1}, T < 240 K can be attributed to lift of degeneration of phonon modes along X direction in the Brillouin zone as a results of deformation of cubic cell. A distinct character of change in modes intensity at lowering of temperature is shown in fig. 2 by dotted lines.

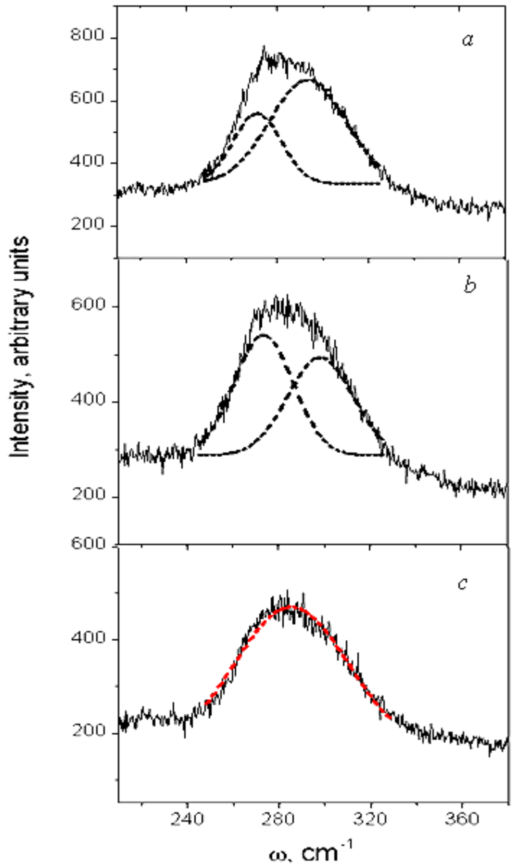

Fig. 2. Raman spectra versus frequency at temperatures of 210 K (*a*), 230 K (*b*), 250 K (*c*) and fitting function for two modes with frequency $\omega_{2,1} \approx$ 272 cm^{-1} and $\omega_{2,2} \approx$ 296 cm^{-1}

Distinction of temperatures, at which feature of characteristic start to manifest by Raman spectra T_{or} = 240K, also exists in the doped manganites.

As T approaches T_{JT}, the structural fluctuations are large enough to break the cooperativeness of the orbital ordering, leading to an average cubic crystal structure at the JT transition [17]. It is interesting to mention that the measured values of the phonon linewidths and intensity for $LaMnO_3$, in particular for the bending and stretching modes, are of the order of those found in amorphous materials, suggesting the existence of a high level of structural disorder at $T > T_{or}$ [17].

Change in the shape of line of Raman spectra is attributed to deformation of cubic structure and lifting degeneration of transverse phonon modes along X direction in the Brillouin zone at $T \leq 240$ K at which is observed the maximum the magnetoelectric effect [18] arisen from formation of orbital order. For $Co_xMn_{1-x}S$ solid solution the average crystal structure is not reveal cooperative distortion of the MnS_6 octahedron at $T > 240$ K. However, above this temperature the short-range orbital ordering may still persist. Below temperature 240 K the degeneration of t_{2g} orbitals is lifted as results of small deformation of octahedron, that leads to splitting phonon modes in the points Brillouin zone. At frequency ω_1, the line is very narrow and its shape and frequency are temperature-independent, while the mode intensity decreases by 20 % and becomes temperature-independent at $T > 230$ K.

References

1. Kugel K. I., Khomskii D. I. Polaron effects and exchange interaction in magnetic insulators with Jahn–Teller ions // Sov. Phys. JETP. 1981. Vol. 52. P. 501–515.
2. Tokura Y., Nagaosa N. Orbital physics in transition-metal oxides // Science. 2000. Vol. 288. P. 462–468.
3. Orbital and charge ordering in $Pr_{1-x}Ca_xMnO_3$ ($x = 0$ and 0,5) from the ab initio calculations / V. I. Anisimov, I. S. Elfimov, M. A. Korotin, K. Terakura // Phys. Rev. B. 1997. Vol. 55. P. 15494–15499.
4. Salamon M. B., Jaime M. The physics of manganites: structure and transport // Rev. Mod. Phys. 2001. Vol. 73. P. 583–628.
5. Sawada H., Terakura K. Orbital and magnetic orderings in localized t_{2g} systems, $YTiO_3$ and YVO_3: comparison with a more itinerant e_g system $LaMnO_3$ // Phys. Rev. B. 1998. Vol. 58. P. 6831–6836.
6. Temperature – induced magnetization reversal in a YVO_3 single crystal / Y. Ren, T. T. M. Palstra, D. I. Khomskii et al. // Nature. 1998. Vol. 396. P. 441–444.
7. Lattice effects in YVO_3 single crystal / C. Marquina, M. Sikora, M. R. Ibarra et al. // JMMM. 2005. Vol. 290–291. P. 428–430.
8. Local lattice distortion during the spin – state transition in $LaCoO_3$ / S. Yamaguchi, Y. Okimoto, Y. Tokura // Phys. Rev. B. 1997. Vol. 54. P. R8666–R8669.
9. Intermediate – spin state and properties of $LaCoO_3$ / M. A. Korotin, S. Yu. Ezhov, I. V. Solovyev et al. // Phys. Rev. B. 1996. Vol. 54. P. 5309–5316.
10. Lattice and charge excitations in $La_{1-x}Sr_xMnO_3$ / P. Bjornsson, M. Rubhausen, J. Backstrom et al. // Phys. Rev. B. 2000. Vol. 61. P. 1193–1197.
11. Order – disorder in the Jahn–Teller transition of $LaMnO_3$: A Raman Scattering study / E. Granado, J. A. Sanjurjo, C. Rettori et al. // Phys. Rev. B. 2000. Vol. 62. P. 11304–11307.
12. Raman spectroscopy of polycrystalline α-MnSe / A. Milutinovic, Z. V. Popovic, N. Tomic, S. D. Devic // Materials Science Forum. 2004. Vol. 453–454. P. 299–304.
13. Measurement and comparative analysis of the second order Raman spectra of the alkaline – eath oxides with NaCl structure / K. H. Rieder, B. A. Weinstein, M. Cardona, H. Bilz // Phys. Rev. B. 1973. Vol. 8. P. 4780–4786.
14. Raman and optical spectroscopic studies of small-to-large polaron crossover in the perovskite manganese oxides / S. Yoon, H. L. Liu, G. Schollerer et al. // Phys. Rev. B. 1998. Vol. 58. P. 2795–2801.
15. Chou H-h., Fan H. Y. Light scattering by magnons in CoO, MnO and α-MnS // Phys. Rev. B. 1976. Vol. 13. P. 3924–3938.
16. Transport properties and ferromagnetism of $Co_xMn_{1-x}S$ sulfides / S. S. Aplesnin, L. I. Ryabinkina, O. B. Romanova et al. // J. of Experimental and Theoretical Physics. 2008. Vol. 106. P. 765–772.
17. Neutron – diffraction study of the Jahn–Teller transition in stoichiometric $LaMnO_3$ / J. Rodrguez-Carvajal, M. Hennion, F. Moussa et al. // Phys. Rev. B. 1998. Vol. 57. P. R3189–R3192.
18. The interrelation of magnetic and dielectric properties of $Co_xMn_{1-x}S$ solid solutions / S. S. Aplesnin, O. N. Bandurina, O. B. Romanova et al. // J. Phys.: Condens. Matter. 2010. Vol. 22. P. 226006–226012.

С. С. Аплеснин, О. Б. Романова, А. С. Крылов, Hsiang-Lin Liu, И. В. Алдашев

ИССЛЕДОВАНИЕ РАМАНОВСКИХ СПЕКТРОВ В ТВЕРДЫХ РАСТВОРАХ $CO_xMnN_{1-x}S$

На твердых растворах $Co_xMn_{1-x}S$ *проведены исследования температурных зависимостей рамановских спектров в интервале частот 100…1 200 см*$^{-1}$ *и температур 100…300 К. Изучение рамановских спектров позволило установить наличие сильных орбитальных флуктуаций в виде сложной формы линии на* $\omega_2 = 273…298$ *см*$^{-1}$*, возникающих в результате расщепления фононной моды с различными температурными зависимостями интенсивности ниже перехода орбитального упорядочения.*

Ключевые слова: магнитно-упорядоченные материалы, рамановские спектры, спин-орбитальный эффект, орбитальные флуктуации, сульфиды.

© Aplesnin S. S., Romanova O. B., Krylov A. S., Hsiang-Lin Liu, Aldashev I. V., 2011